

PNV5203 – Interação Fluido Estrutura I

Galloping



**ESCOLA POLITÉCNICA DA UNIVERSIDADE DE SÃO PAULO
DEPARTAMENTO DE ENGENHARIA NAVAL E OCEÂNICA**

Galloping

ORIGEM

Recolamento

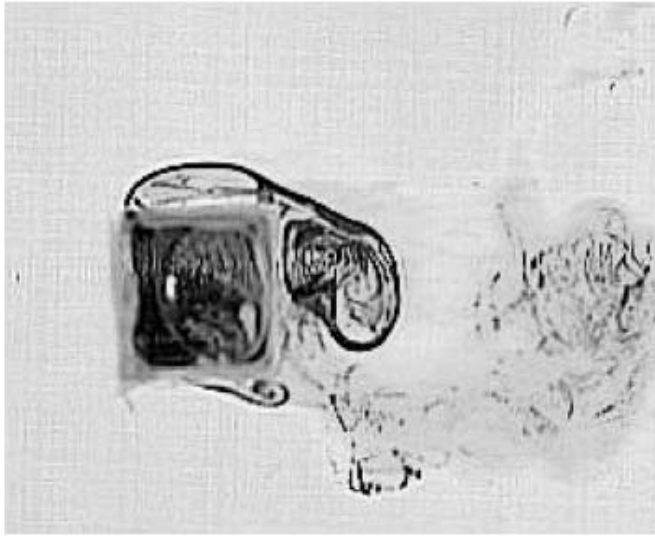


Fig. 18. A weak reattachment of the upper shear layer at $Re = 1000$, $\alpha = 2^\circ$.

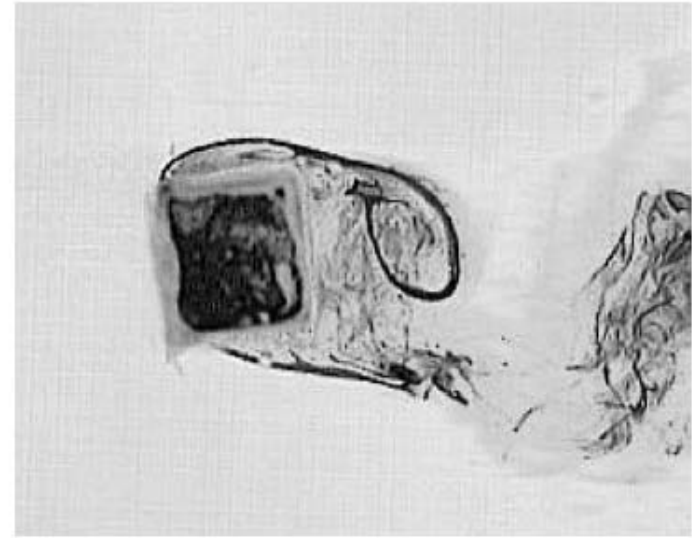


Fig. 19. A weak reattachment of the upper shear layer at $Re = 1000$, $\alpha = 6^\circ$.

Luo, S. C., Chew, Y., & Ng, Y. T. (2003). Hysteresis phenomenon in the galloping oscillation of a square cylinder. *Journal of Fluids and Structures*, 18

Recolamento

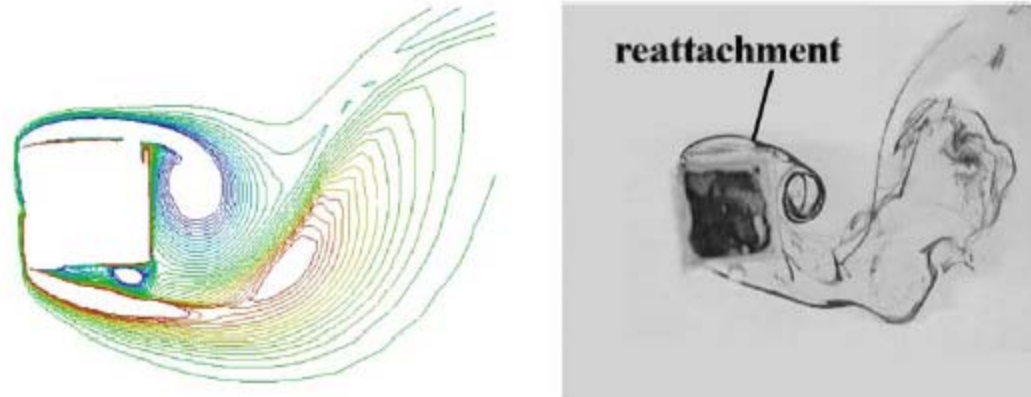


Fig. 16. Comparison between numerical and experimental flow visualization at $Re = 1000$, $\alpha = 4^\circ$. A reattached upper shear layer is seen.

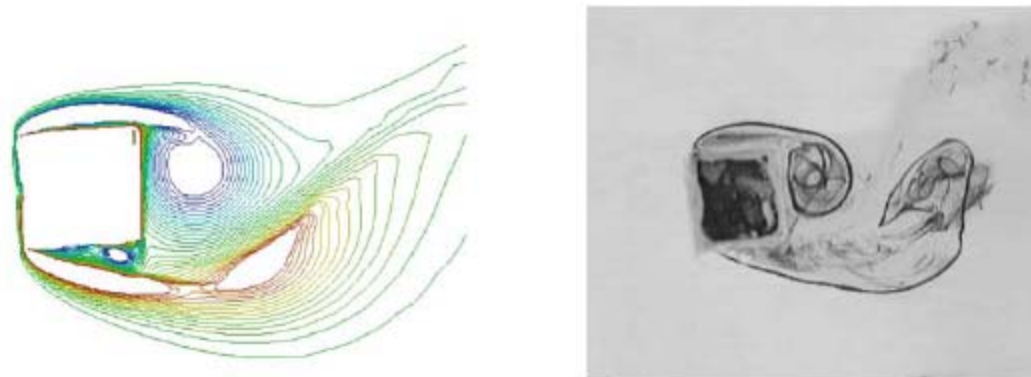
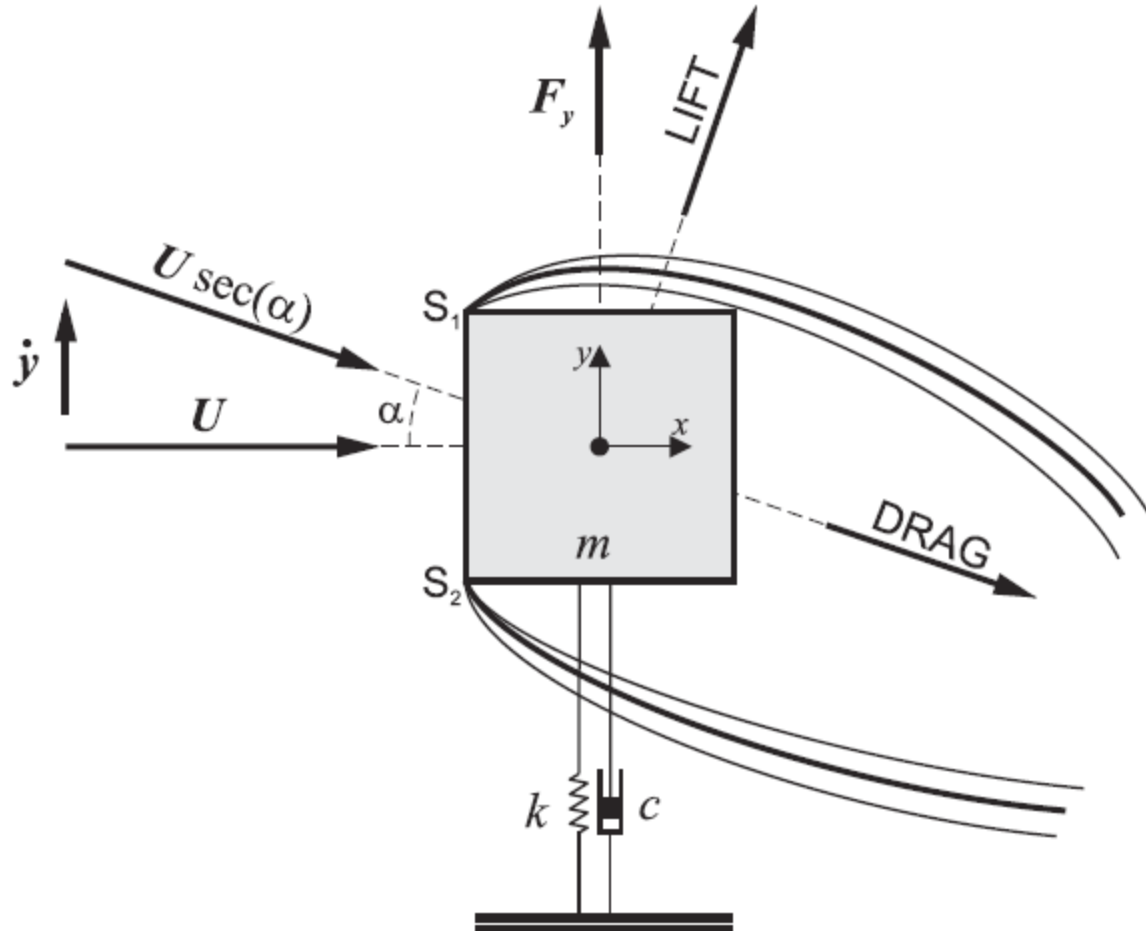


Fig. 17. Comparison between numerical and experimental flow visualization at $Re = 1000$, $\alpha = 4^\circ$. No reattachment of the upper shear layer is seen.

Luo, S. C., Chew, Y., & Ng, Y. T. (2003). Hysteresis phenomenon in the galloping oscillation of a square cylinder. *Journal of Fluids and Structures*, 18

Galloping de seção quadrada



Distribuição de pressão nas faces

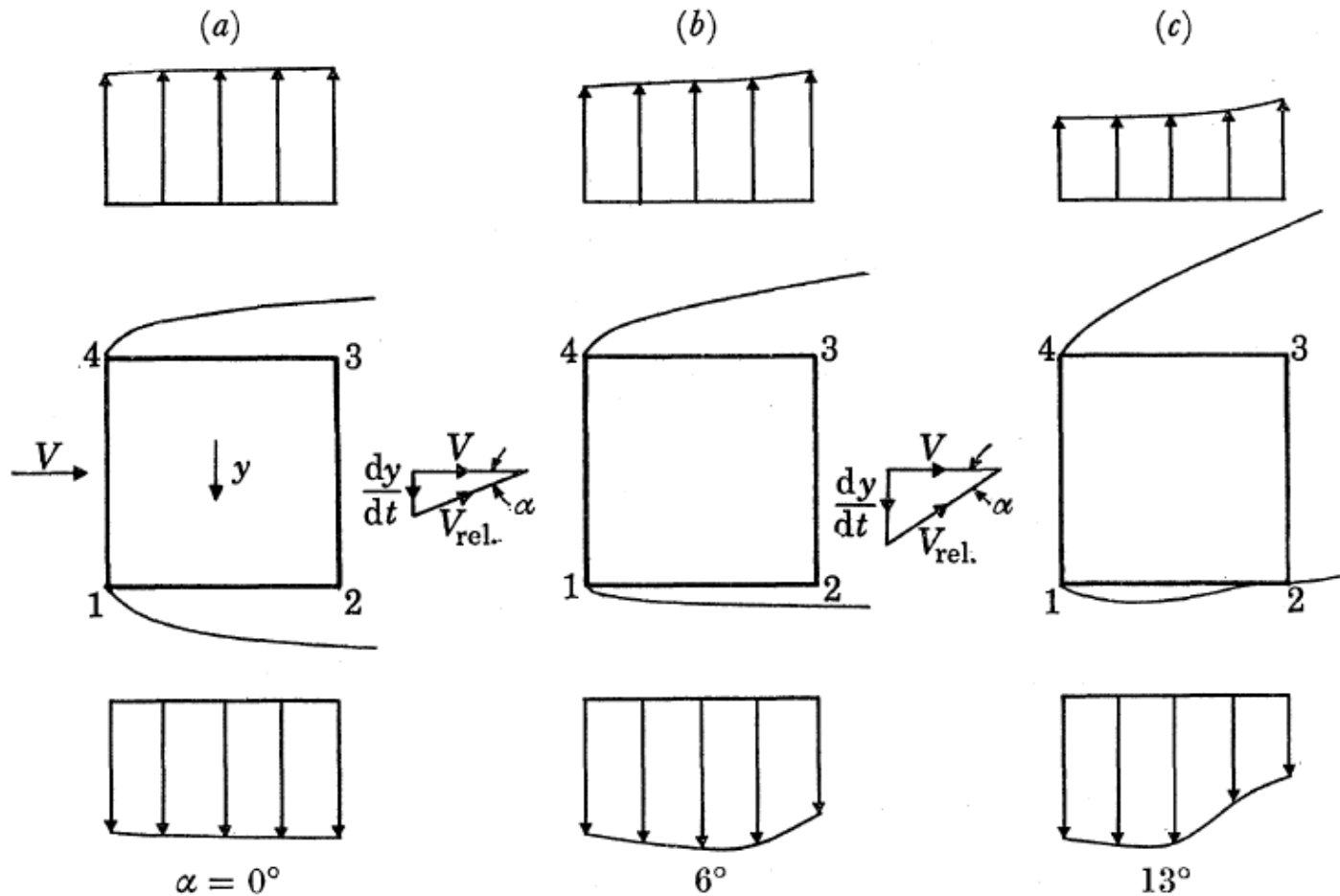
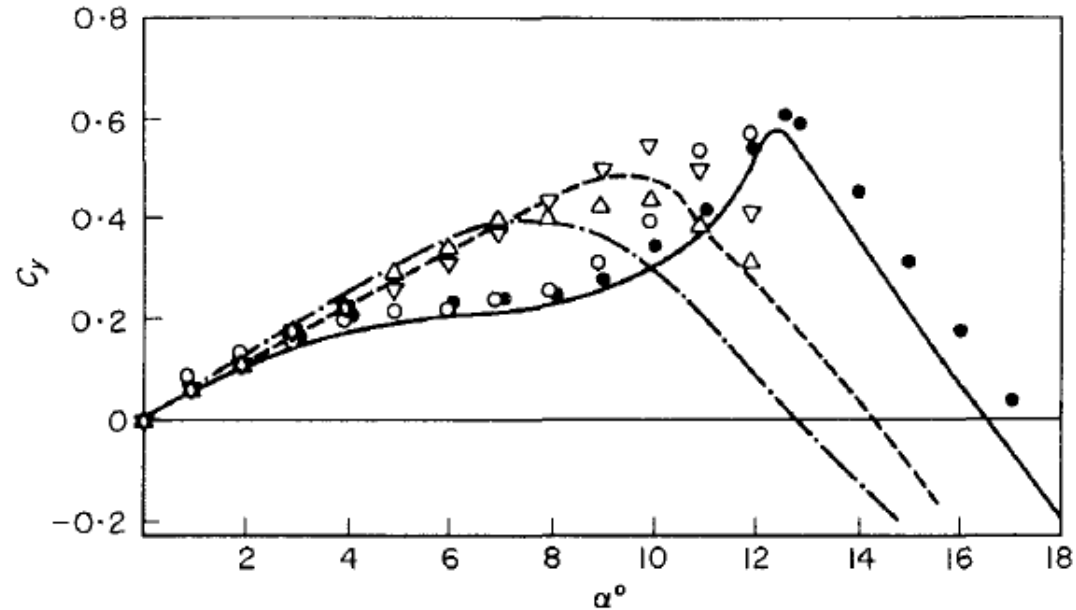


FIGURE 7. Effects of square section afterbody on separated shear layers during galloping. Pressure distributions on sides are shown to scale.

Força vertical para seção quadrada



Source	Turbulence								
	Low		Medium		High				
	Re x 10 ⁻³	v'/v %	Re x 10 ⁻³	v'/v %	Re x 10 ⁻³	v'/v %			
Present data	o	14	0	∇	14	6.5	Δ	14	10.5
Smith [1]	—	22	0						
Wawzonek [5]	•	12	0						
Laneville [14]				---	32	6.7	·-·-	32	12

Figure 5. Lateral force coefficients for square section.

Bearman, P., Gartshore, I., Maull, D., & Parkinson, G. (1987). Experiments on flow-induced vibration of a square-section cylinder. *Journal of Fluids and Structures*, 1

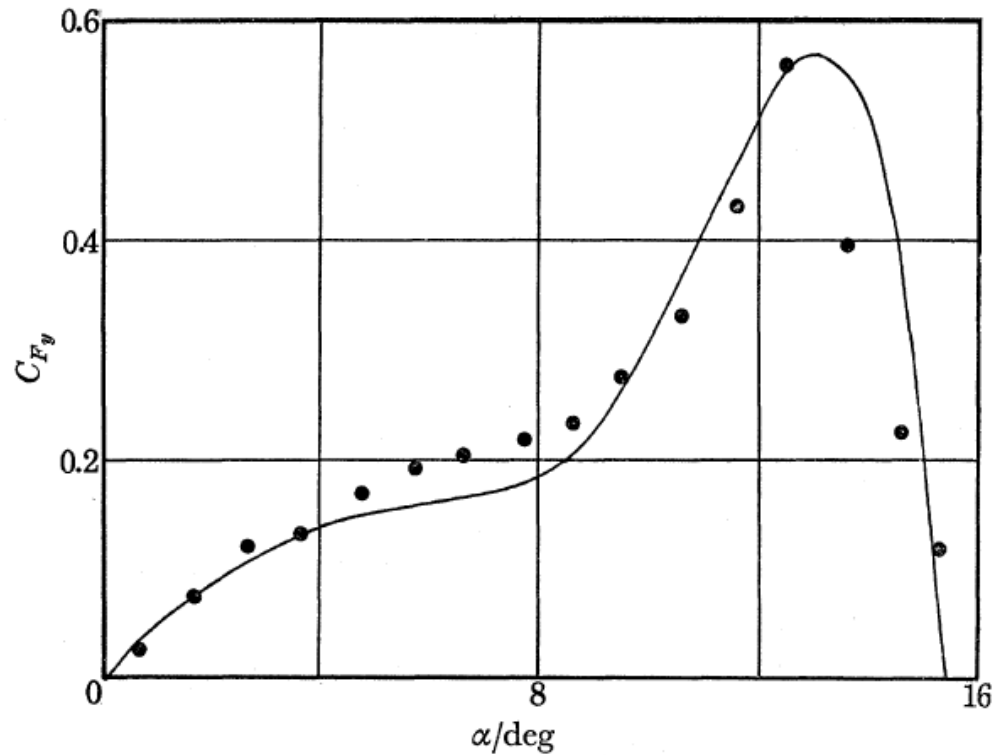
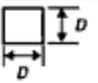
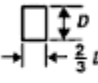
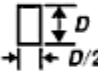
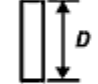
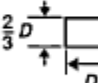
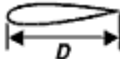
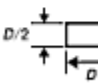

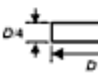

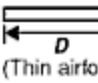
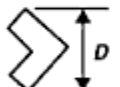


FIGURE 8. Transverse force coefficient C_{F_y} as a function of angle of attack α for square section. ●, experimental points (Smith 1962), $Re = 22\,300$; —, polynomial approximation (Parkinson & Smith 1964).

Table 2.1. The transverse force coefficient^a for various sections in steady smooth or turbulent flow (after Blevins (1990))

Section	h/d	$\partial C_{F_y} / \partial \alpha$		Reynolds number					
		Smooth flow	Turbulent flow ^b						
	1	3.0	3.5	10^5					
	3/2	0.	-0.7	10^5					
	2	-0.5	0.2	10^5					
	4	-0.15	0.	10^5					
	2/3	1.3	1.2	6.6×10^4		-	-6.3	-6.3	$> 10^3$
	1/2	2.8	-2.0	3.3×10^4		-	-0.1	0.	6.6×10^4
	1/4	-10.	-	$2 \times 10^3 - 2 \times 10^4$		-	-0.5	2.9	5.1×10^4
 (Thin airfoil)	- ^c	-6.3	-6.3	$> 10^3$		-	0.66	-	7.5×10^4

^a α is in radians; flow is left to right. $\partial C_{F_y} / \partial \alpha = -\partial C_L / \partial \alpha - C_D$, with C_{F_y} based on the dimension D , so that $\partial C_{F_y} / \partial \alpha > 0$ for galloping.

^b Approximately 10% turbulence.

^c Inappropriate to use h/d .

Galloping

RESPOSTA

Resposta da seção quadrada

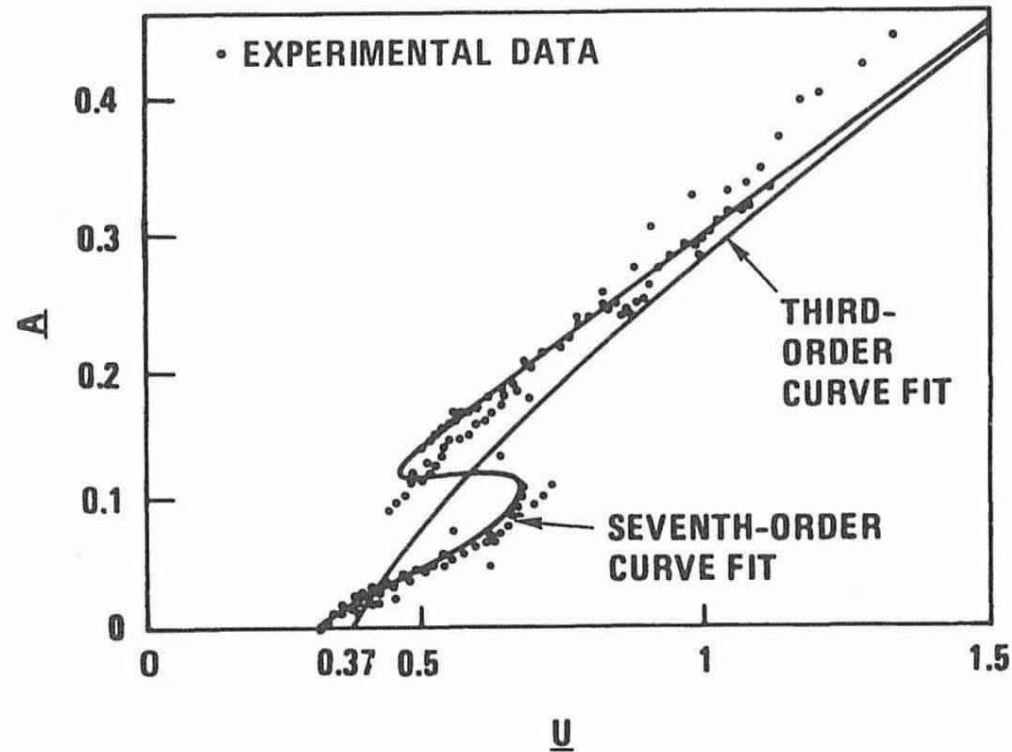


Fig. 4-6 Experimental data and response of a square section (Fig. 4-1). $Re = 4000$ to $20\,000$ (After Parkinson and Smith, 1964).

Resposta da seção quadrada

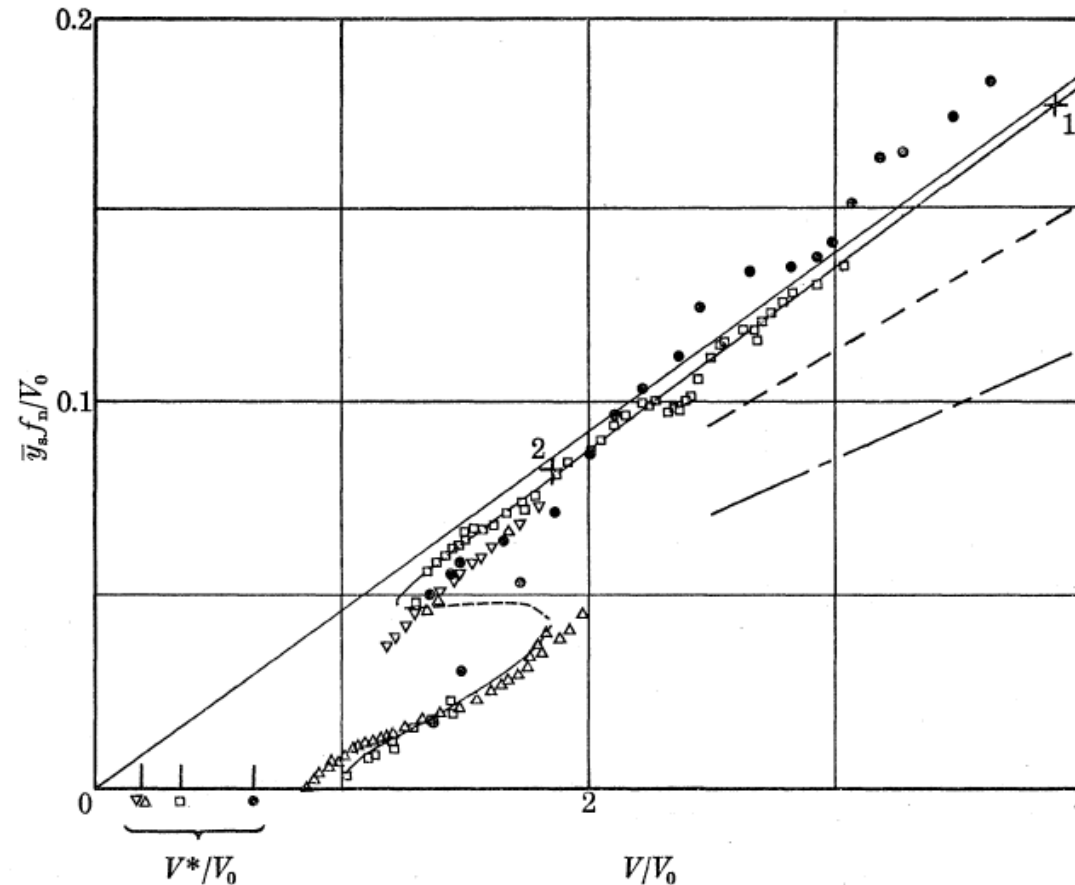


FIGURE 9. Reduced galloping amplitude $\bar{y}_n f_n / V_0$ as a function of reduced wind speed V/V_0 for square section. Experiments (Smith 1962): ●, $\beta = 0.00107$; □, $\beta = 0.00196$; △, $\beta = 0.00364$; ▽, $\beta = 0.00372$; +1, $\beta = 0.0012$; +2, $\beta = 0.0032$. $4000 < Re < 20000$. $n = 0.00043$. Theory (Parkinson & Smith 1964): —, stable limit cycle; ----, unstable limit cycle. Experiments (Novak 1968): - - - - - , 4.7% turbulence; - - - - - - - , 8.6% turbulence.

Possível resposta

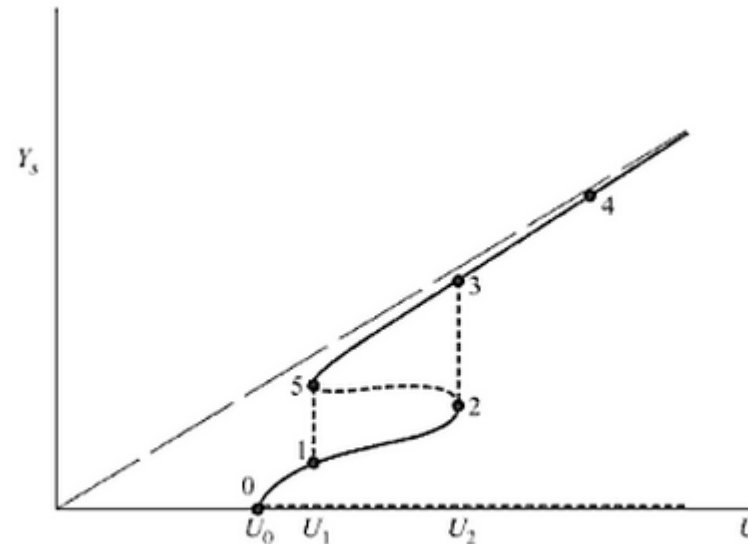


Figure 2.9. Galloping amplitude versus flow velocity, showing the various bifurcations and the “oscillation hysteresis” [from Parkinson & Smith (1964)]; $U_0 = U_{cr}$.

- (i) for $U < U_{cr} \equiv U_0$, only the trivial $R = 0$ solution exists, and the system is stable ($dR/d\eta < 0$);
- (ii) for $U_0 < U < U_1$ and for $U > U_2$ two roots are found, one of which corresponds to a stable limit cycle, whereas the trivial solution is now unstable;
- (iii) for $U_1 < U < U_2$ four roots are found, involving (a) the unstable source at the origin of the phase plane, (b) a stable limit cycle nesting within (c) an unstable one, which in turn nests within (d) a larger stable limit cycle.

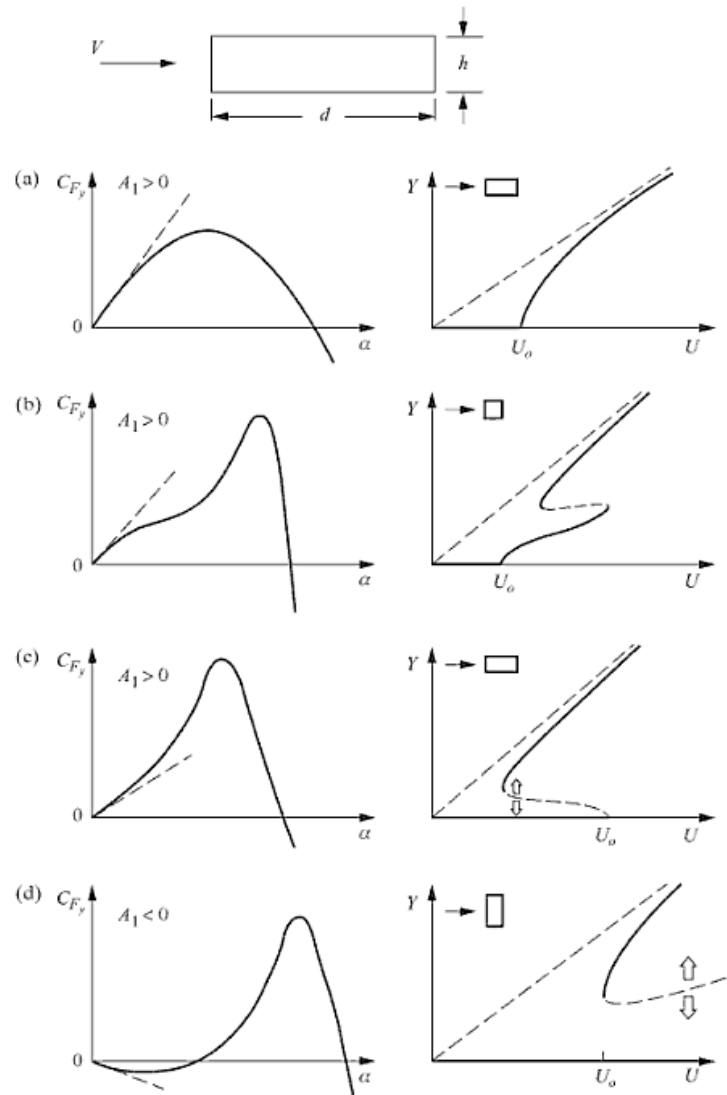
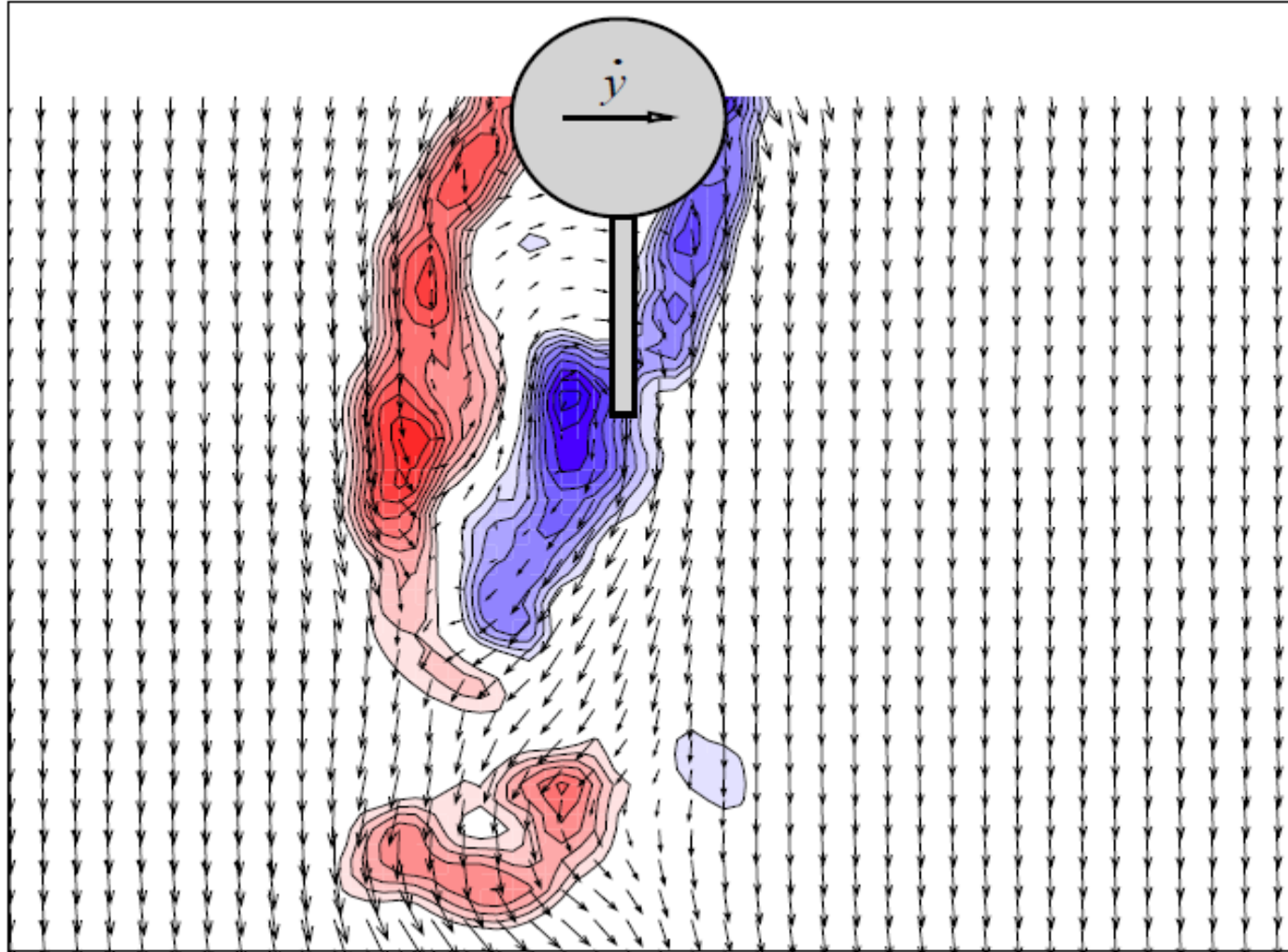


Figure 2.12. Typical lateral force coefficients and corresponding types of galloping response for prisms of different height, h , and depth, d ; $Y = a/h$ and $U = V/\omega h$; from Novak (1971).

Galloping

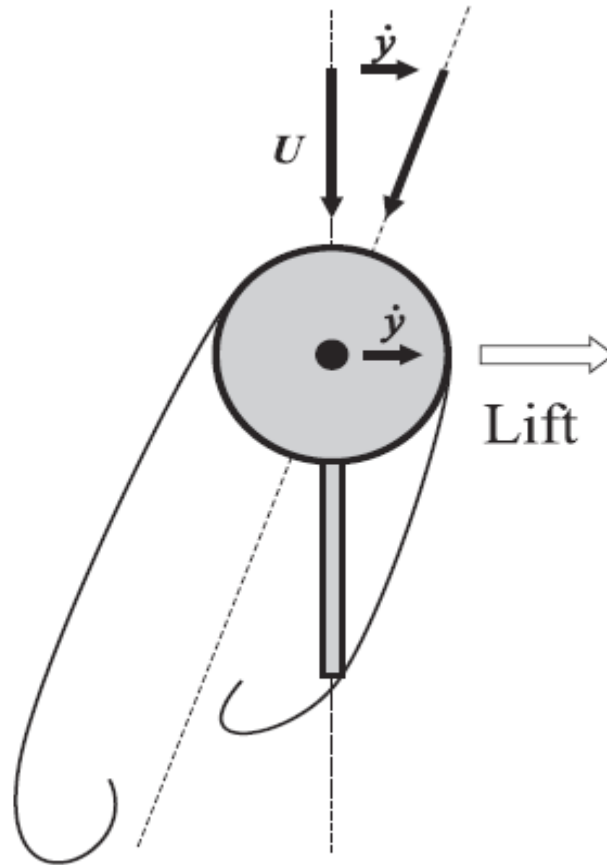
CILINDRO COM PLACA PLANA

Cilindro com placa plana

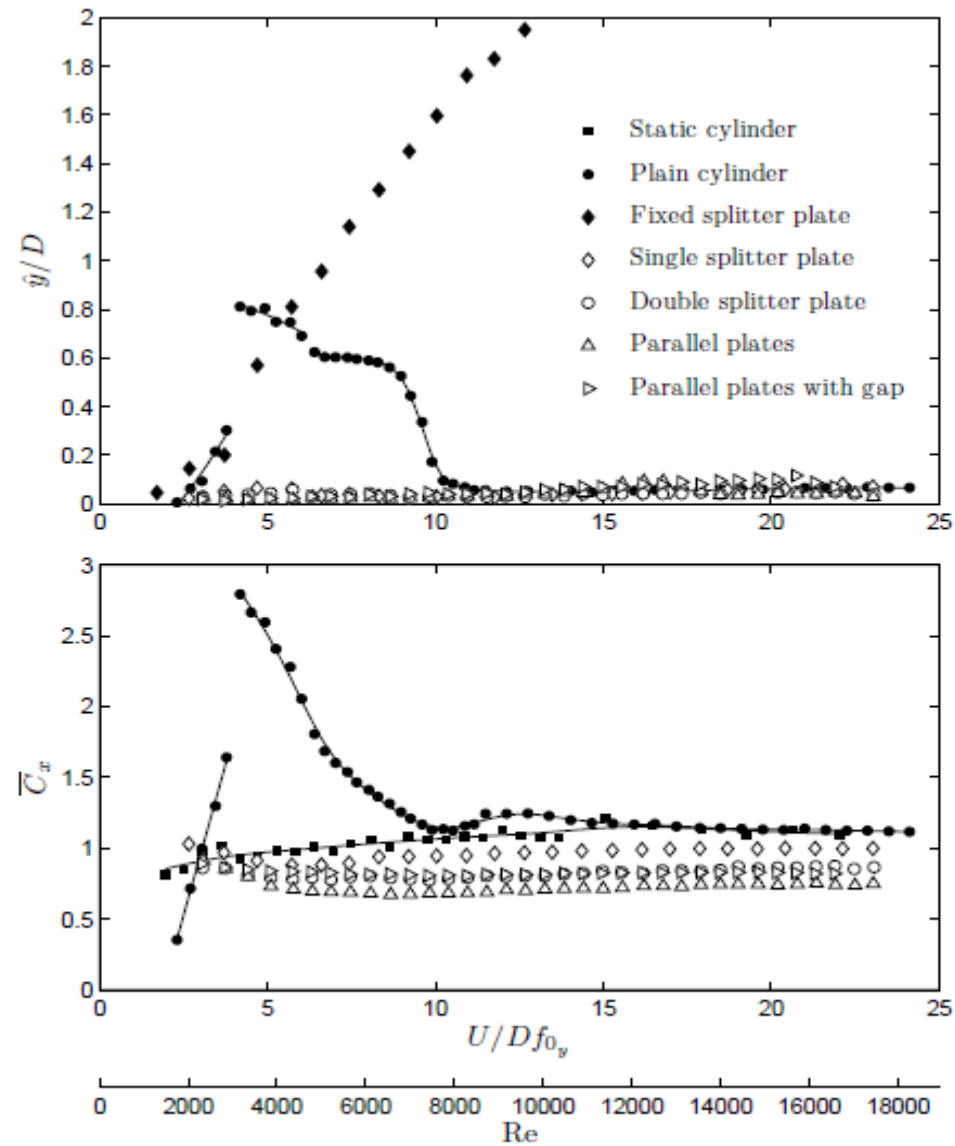


Assi, G.R.S. (2009). *Mechanisms for flow-induced vibration of interfering bluff bodies*. PhD Thesis, Imperial College London

Cilindro com placa plana

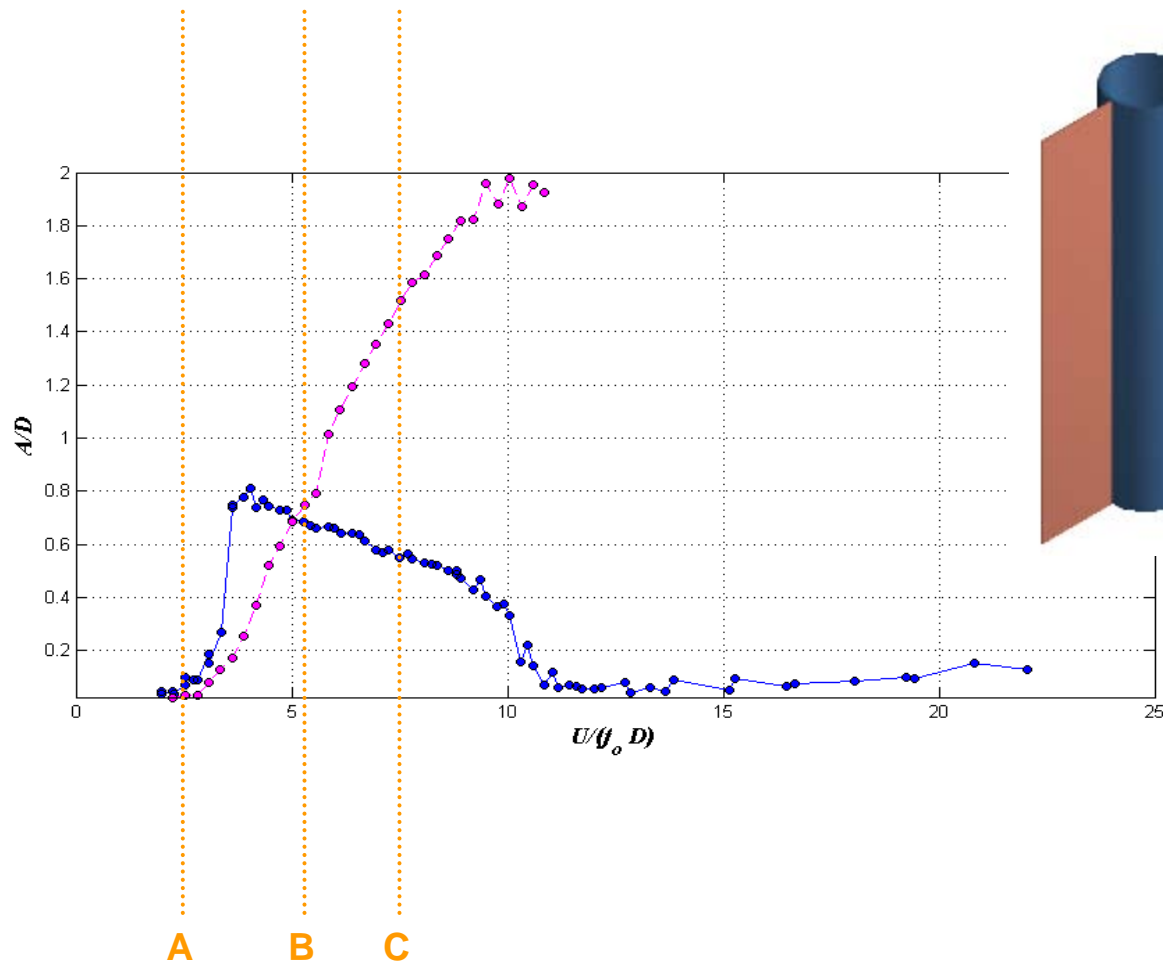


Assi, G.R.S. (2009). *Mechanisms for flow-induced vibration of interfering bluff bodies*. PhD Thesis, Imperial College London



Assi, G.R.S. (2009). *Mechanisms for flow-induced vibration of interfering bluff bodies*. PhD Thesis, Imperial College London

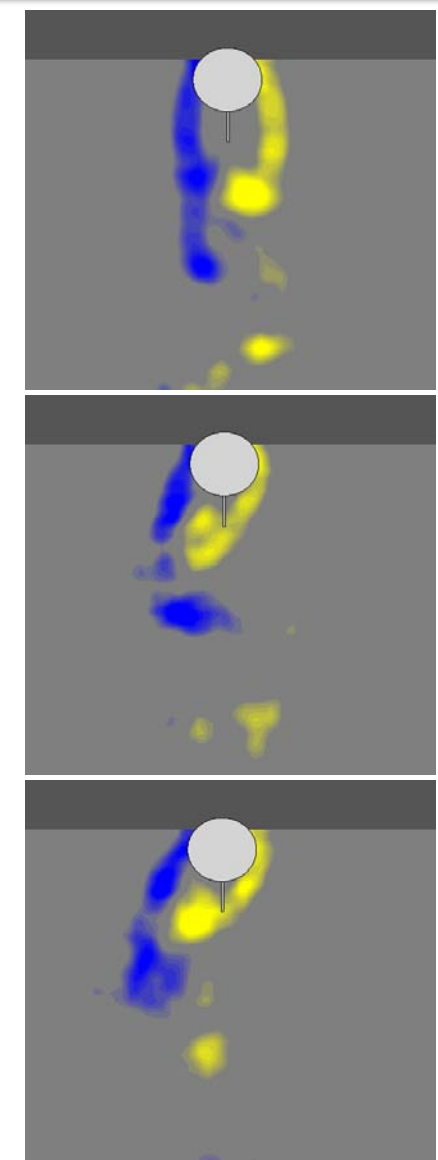
Splitter plate 0.5D



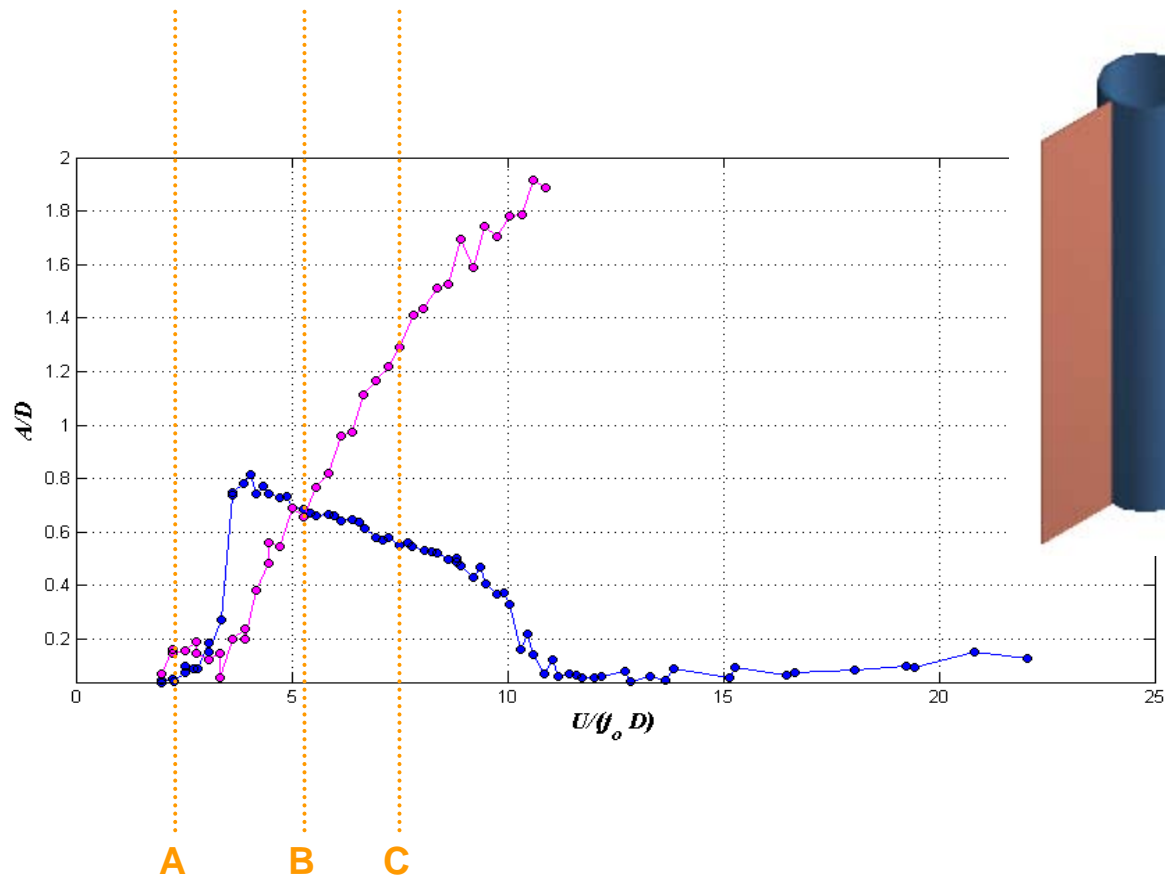
A

B

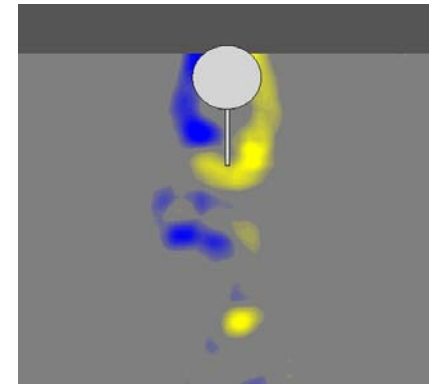
C



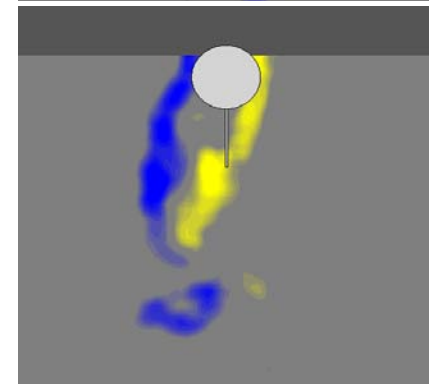
Splitter plate 1.0D



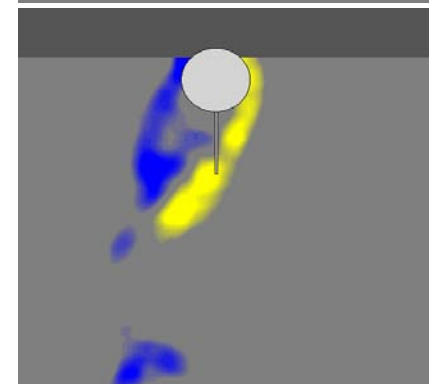
A



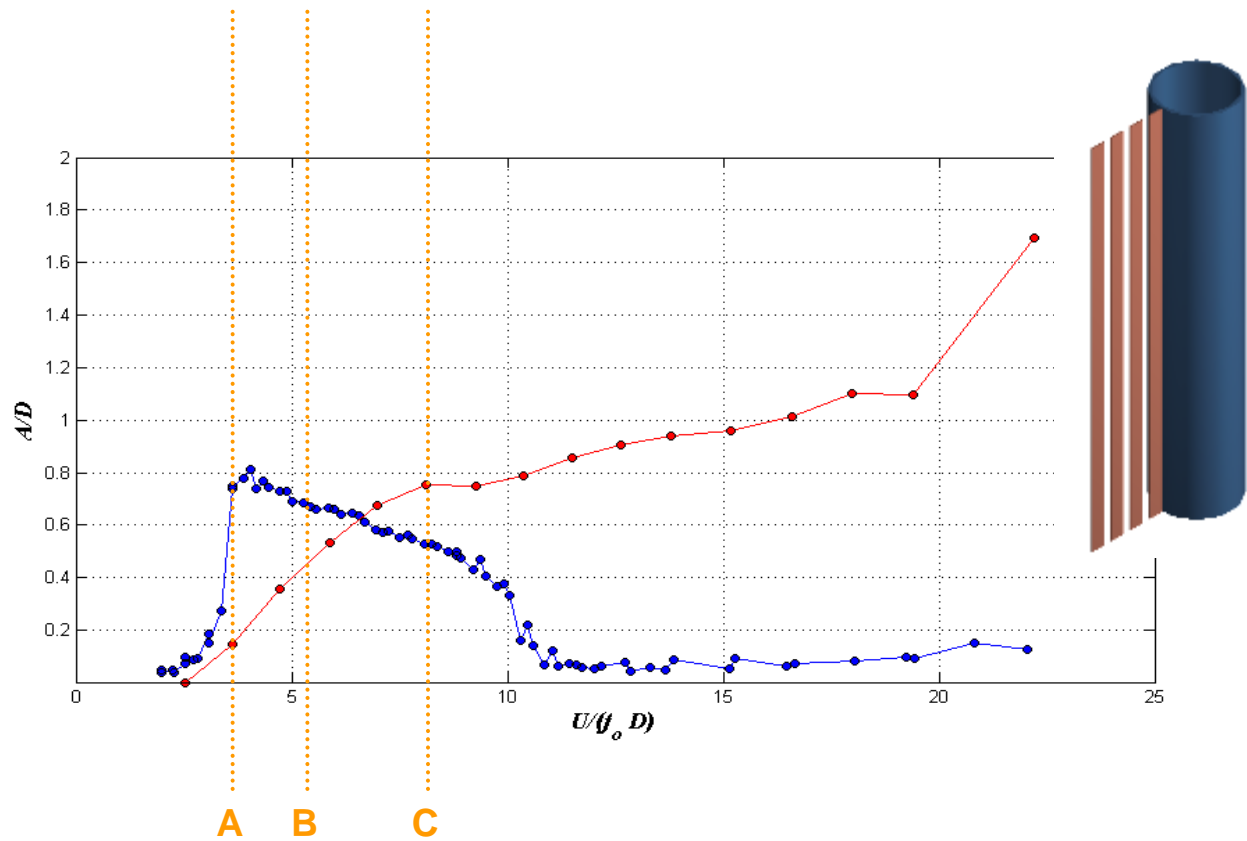
B



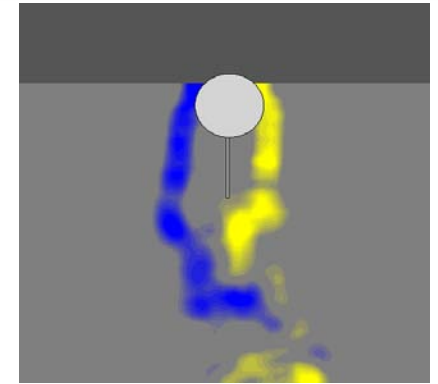
C



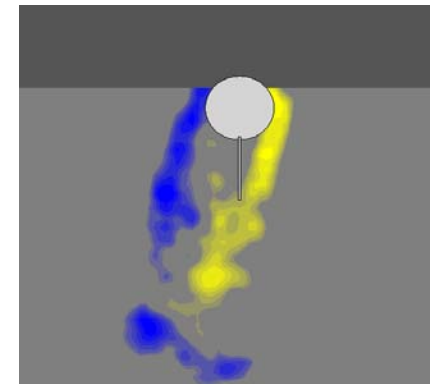
Slotted plate 1.0D



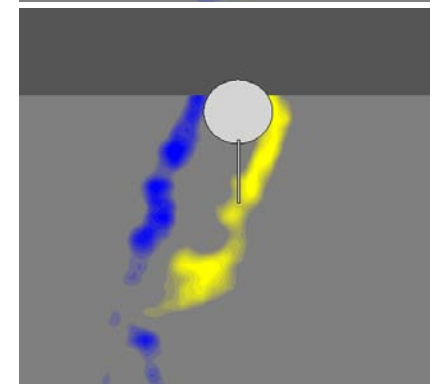
A



B

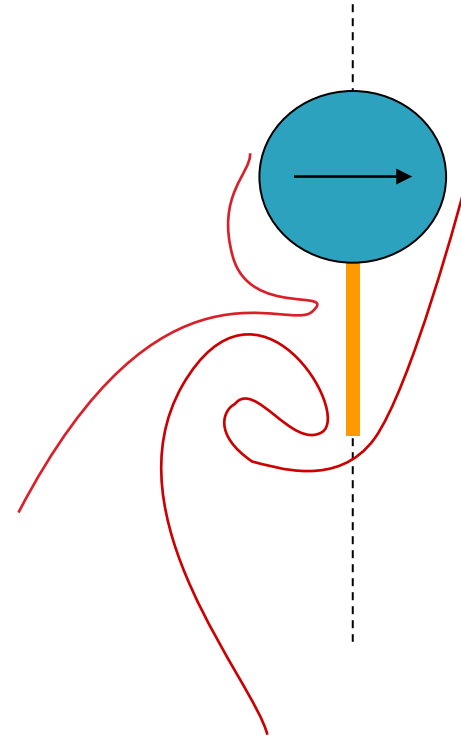
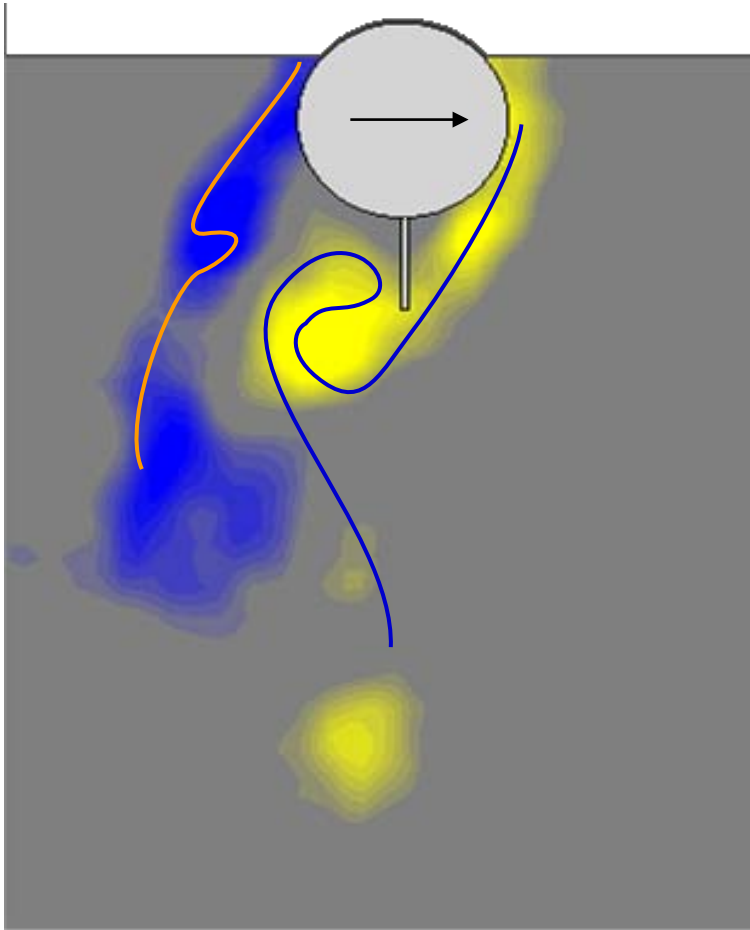


C



Assi, G.R.S. (2009). *Mechanisms for flow-induced vibration of interfering bluff bodies*. PhD Thesis, Imperial College London

Galloping mechanism



Assi, G.R.S. (2009). *Mechanisms for flow-induced vibration of interfering bluff bodies*. PhD Thesis, Imperial College London

